

# The Impact of Diffuse Illumination on Iris Recognition

Amanda Sgroi, Kevin W. Bowyer, and Patrick J. Flynn  
University of Notre Dame

asgroi kwb flynn @nd.edu

## Abstract

*Iris illumination typically causes specular highlighting both within the pupil and iris. This lighting variation is intended to be masked in the preprocessing stage. By removing or reducing these specular highlights, it is thought that a more accurate template could be made, improving the matching results. In an attempt to reduce these specular highlights we propose a diffuse illumination system. To determine if iris recognition performance is enhanced by this diffuse illumination system, we examine whether specular highlights were reduced within the pupil and iris, as well as analyze matching results obtained by several iris algorithms.*

## 1. Introduction

Iris recognition began with visibly illuminated frames from a video stream [4]. Since Daugman's first iris segmentation and recognition experiments, the field has advanced to using images that are illuminated by light sources of various spectra, from visible to near infrared (NIR). Due to the nature of these new illumination systems, standards are now being imposed in order to best protect subjects during acquisition [1]. However, one major artifact of iris illumination which can cause variations in both the segmentation and recognition is specular highlighting. In this study we will present a new diffuse illumination system for reducing the effects of specular highlights.

### 1.1. Image Quality and Illumination

Surveys of iris biometrics identify illumination as one factor with great impact on image quality [3][5]. Image quality is a function of many factors including lighting as well as focus, occlusion, and other sensor imposed artifacts. The use of NIR illumination has proved advantageous over visible illumination for iris imaging in many ways. NIR illumination produces images with more distinct texture across a larger range of iris pigments, and cannot be perceived by the human eye, thus aiding in the control of

pupil dilation. Yet, specular highlights from the illumination still appear within images of the iris.

In this study, we aim to reduce the effects of specular highlights by introducing diffused illumination to the LG IrisAccess 4000 sensor. By diffusing the illumination provided by this sensor, we hope to reduce the strength and number of specular highlight pixels found within both the pupil and the iris, an illumination technique not currently employed by commercial iris sensors. Through the acquisition process of this modified system, we hope to achieve a better iris template by improving the segmentation and increasing the number of unoccluded pixels.

## 2. Designing a Diffuse NIR System

### 2.1. LG IrisAccess 400

The LG IrisAccess 4000 captures images of both eyes at the same time [7]. Inspection of the sensor reveals that it makes use of two clusters of near-infrared light-emitting diode illuminators of varying spectra which provide cross and direct illumination of both irises [6]. For acquisition to occur, a subject must be approximately 14 inches away from the sensor, with eyes centered in the reflective acquisition window. During each acquisition session, multiple sets of iris image pairs are taken.

### 2.2. The Diffuse Illumination System

In this study, the LG 4000 was chosen as the sensor to alter due to its availability in our lab, as well as the sensor being representative of current commercial sensors. The LG IrisAccess 4000 uses 12 NIR LEDs on both the left and right side of the sensor. Five of the LEDs on each side, closest to the center of the sensor, are placed perpendicular to the surface of the sensor, and are used for direct illumination of the iris such that LEDs on the right side of the camera illuminate the right eye, and vice versa. The other seven LEDs are placed at an angle, and are used for cross illumination of the iris such that LEDs on the right side of the camera illuminate the left eye, and vice versa. Wavelengths of both 770 nm and 870 nm are used to achieve the desired level of iris texture for various ranges in iris coloring [6].

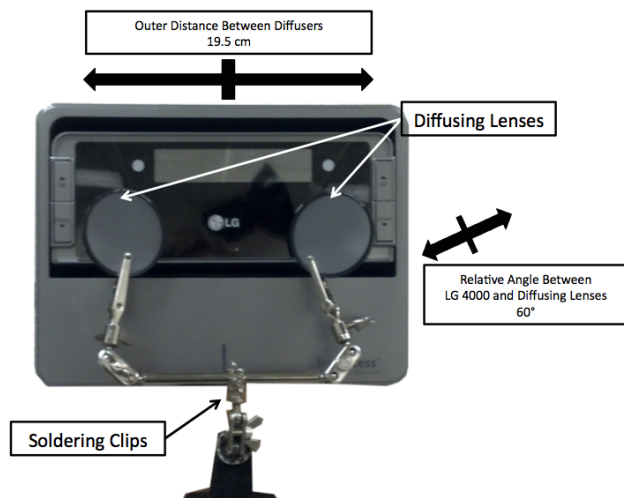


Figure 1. Diffuse Illumination System Setup Diagram showing the distance between the diffusers as well as the relative angle between the diffusing lens and LG 4000 sensor.

The original configuration of the LG IrisAccess 4000 places a tinted plate of glass in front each LED cluster. In order to diffuse the produced illumination, a set of diffusing lenses produced by Edmund Optics were purchased and positioned carefully in front of the LED clusters on the outside of the sensor [2]. These lenses are 25 mm circular pieces of sandblasted glass, all with a transmission efficiency greater than 85%. Three levels of diffusion were used in this study, namely 20, 25, and 30 degrees, based on an earlier smaller study. The level of diffusion describes the angle at which light entering perpendicular to the lens will leave after passing through it. Each lens diffuses light in a spectral range from 400 nm to 1600 nm, which includes the NIR spectrum provided by the sensor.

In order to create our diffuse illumination system, a set of two lenses of the same degree of diffusion were used. Clips secured by a base were used to position and hold the lenses in place over each LED cluster. The lenses are placed several inches away from each other's center, and at an angle towards the center of the sensor, as shown in Figure 1. By placing them at this location and angle, we assured that all illuminators were covered and that both direct and cross illumination were affected without compromising the proximity sensors, as shown in Figure 1. During the acquisition process, an unaltered LG IrisAccess 4000 was used to acquire images of a subject's irises first, followed by images of the same irises using a separate LG IrisAccess 4000 with the diffuse illumination system in order to best compare the two systems.

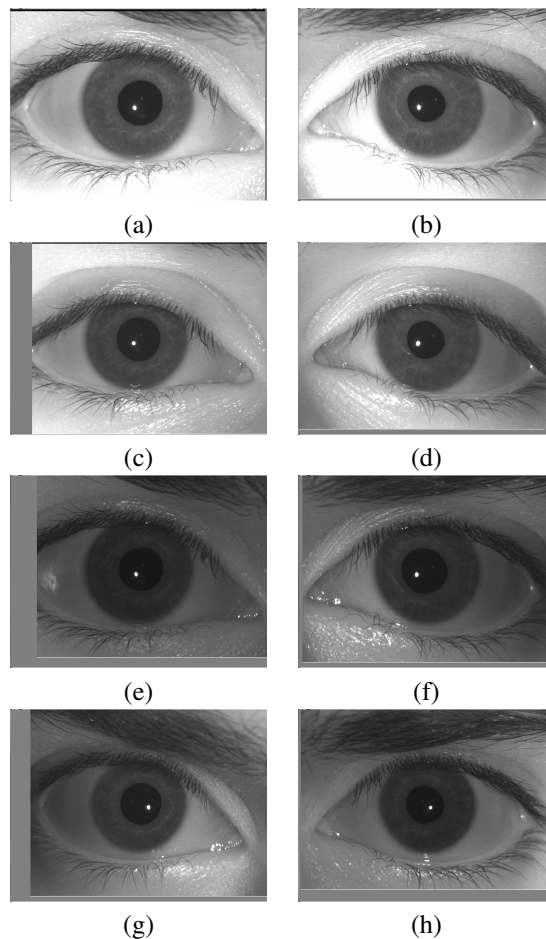


Figure 2. Right (a) and Left (b) eyes from traditional illumination. Right (c) and Left (d) eyes from 20 degrees of diffuse illumination. Right (e) and Left (f) eyes from 25 degrees of diffuse illumination. Right (g) and Left (h) eyes from 30 degrees of diffusion. All images are from subject nd1S06005 across various sessions.

### 3. Dataset

The data collected using the unaltered LG IrisAccess 4000, labeled as "traditional" in the remainder of this study, and the diffuse illumination system, was gathered over 6 months from November 2010 to April 2011. Each set of illuminators was used in two different sessions, which extended over a period of three days. The positioning of the lenses was checked periodically to ensure consistency of illuminations by the diffuse system. Table 1 describes the breakdown of images and subjects per session across the study. A noticeable variation is found in the lack of images and subjects between the diffuse and traditional categories for session 4. This was due to a loss of one day's worth of data due to technical errors. Other, smaller variations between the number of images and subjects between the two categories are due to failures to enroll with a particu-

	Degree of Diffusion	Number of Diffused Images	Number of Traditional Images	Number of Diffused Subjects	Number of Traditional Subjects
Session 1	25 °	1106	1095	287	287
Session 2	30 °	1230	1835	287	339
Session 3	30 °	1122	1703	234	208
Session 4	20 °	702	1624	90	205
Session 5	20 °	1999	1999	251	252
Session 6	25 °	1897	1918	239	242

Table 1. Subject Breakdown by Session

lar sensor. In all cases, the diffuse illumination system has somewhat smaller image counts, which can be attributed to a possible disruption in proximity due to small movements of the diffusing lenses by subjects and operator movement around the device.

Figure 2 shows images from the different acquisition scenarios. The top row shows the traditional illumination results. The level of diffuse illumination increases down the columns from 20 to 25 to 30. As the level of diffusion increases, the contrast in each image is lessened. Additionally, the diffused images often have more padding, the gray borders, along the sides of the image. This is due to how the sensor zooms and crops the image during the acquisition process to assure the correct size and average iris area in each image. These, and other quality variations, are examined later.

## 4. Reduction of Specular Highlights

Specular highlights may occur within the pupil and/or within the iris. By reducing specular highlights within the pupil, particularly highlights close to the pupillary boundary, we can improve pupil detection and segmentation. Similarly, by reducing specular highlights near the scleral boundary, we may improve the detection and localization accuracy of that boundary. Additionally, by reducing the specular highlights in the iris, we may reduce the number of masked pixels, potentially improving the template created by an image segmenting and matching algorithm.

### 4.1. Within the Pupil

In order to determine whether specular highlighting was reduced within the pupil, average histograms of all pupils were generated. Specifically, the segmentation information provided by Algorithm 3, as discussed in Section 5.3, preprocessing stage was used to examine the pixel data from inside the pupil. These pixel intensities were found for each image category per week, and plotted in a normalized histogram for comparison. Figure 3 shows the resulting histograms from the traditional and diffuse illumination systems per session. The x-axis of the histograms represents pupil intensity, where 0 is black, and 255 is white. In the traditional illumination histograms, almost all of the his-

tograms are centered around 50, with a small peak around 125, and larger peak at 255. Comparatively, in the diffused illumination histograms the largest peak is centered to the left of 50, no peak is found around 125, but a peak is still seen at 255. These peaks at 255 represent the strength of the specular highlight. The small peaks at 125 in the traditional histograms represent the halo around the strongest point of the specular highlight. The fact that this type of peak is not present in the diffused illumination pupil histograms proves that the effect of specular highlighting has been reduced. Further, the largest peak being shifted to the left in the diffused illumination graph speaks to the fact that the contrast is darker in the diffused images.

### 4.2. Within the Iris

To analyze the resulting specular highlights within the iris texture, connected components were used to describe highlight regions' pixels. Using the segmentation information provided by the preprocessing stage of Algorithm 3, the iris region alone was extracted from each image. A histogram of all the pixels in this region was then developed. The top 3% of pixels closest to white were considered to fall around a specular highlight component. A mask of only these pixels was then used to determine connected components of an appropriate size which best described the specular highlights. Components which were too large were excluded since this often is descriptive of eyelid and eyelash occlusion. In contrast, regions which were too small were eliminated since these may describe the iris texture. Many iris recognition algorithms provide their own methods for segmentation and masking occlusion and specular highlights. Since Algorithm 3's preprocessing information was used, our results were compared to the results of this algorithms' segmentation and masking.

Figure 4 (a) shows a comparison in the number of connected components found during diffuse illumination acquisition compared to the number of connected components found during traditional acquisition. The means in these boxplots are all maintained around two. This is due to the illumination pattern placed on the eye which often causes highlights at the extreme top and bottom of the iris from reflections off the eyelid. Other specular highlights can often

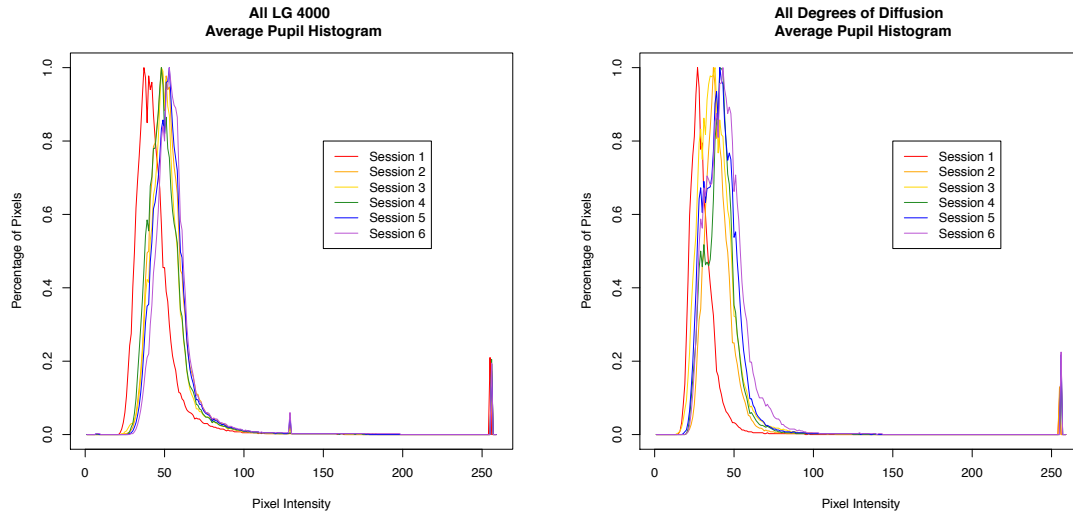


Figure 3. Traditional Pupil and Diffused Pupil Histograms.

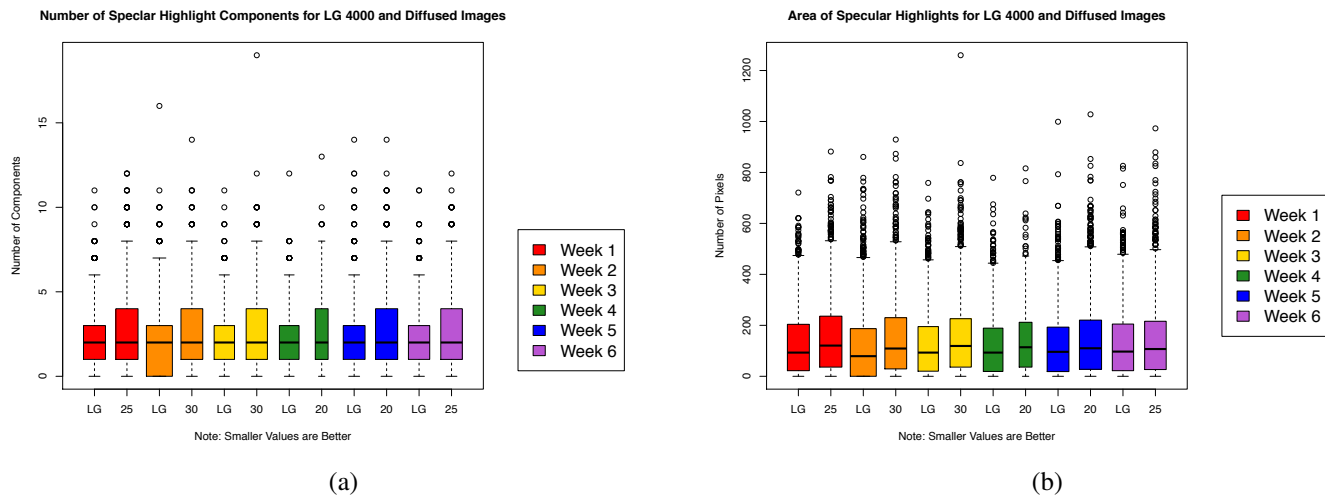


Figure 4. Traditional Iris and Diffused Iris Specular Highlight boxplots. Here 20, 25, and 30 refer to degrees of diffusion used for the represented subset of data. Similarly, LG refers to a traditionally illuminated subset of data. (a) The number of specular highlight connected components were found within the iris. (b) The sum of the area these components occupied within the irises.

be found on the pupillary boundary and elsewhere throughout the iris. Some specular highlights can even be caused by reflections off the nose. Although we appear to not be reducing the number of specular highlight components, we are not increasing them on average when using diffuse illumination. The increase in standard deviation is most likely due to differences in contrast.

In Figure 4 (b), we further illustrate the impact of specular highlights in the iris region by comparing the number of pixels found which describe a specular highlight. The av-

erage area consumed by specular highlights within the iris region for all cases is around 125 pixels. We find no statistically significant difference in the means between traditional and diffused data, such that mean of the diffused data falls within one standard deviation of the traditional data. This is consistent with the number of specular highlights found. However, it does seem that we are not reducing the impact of specular highlights as much within the iris as within the pupil when using diffuse illumination. Testing in a recognition scenario will further explore the results of our diffuse

illumination system.

## 5. Effects of Diffuse Illumination on Iris Recognition

Since each algorithm available for use employs a different segmentation and matching method, each was used to analyze the results of the diffuse illumination system. In particular, given the diffuse and traditional dataset, for each algorithm, templates were made and three different types of experiments were performed. In the first experiment, the probe and gallery sets contained images acquired from the diffuse illumination system. Similarly, in the second experiment, the probe and gallery sets contained images acquired from the unaltered LG IrisAccess 4000. The third type of experiment used the traditional LG IrisAccess 4000 images as the gallery and the diffuse images as the probe set. Due to the fact that two of the matching algorithms provide asymmetric scoring, in the experiments which compare the same type of illumination, the older of the two image sets was used as the gallery set.

### 5.1. Algorithm 1

Algorithm 1 is a commercial SDK, which outputs an asymmetric distance score which ranges from zero to approximately one, where zero indicates a perfect match. Figure 5 shows ROC curves for the three types of experiments performed on the diffuse and traditionally illuminated data. Each experiment is labeled as "Session XvY", meaning that images from Session X formed the gallery set and images from Session Y formed the probe set. The figure (a) shows comparisons performed within a single session between diffuse illumination images and traditional illumination images. All six experiments have mean ROC results between a true accept rate of 0.985 and 0.975 at a false accept rate of 0.002. Further, all error bars are overlapping. Thus it is unlikely that the results of these experiments are statistically significantly different from one another. Hence, the performance of each experiment of various levels of diffusion is similar.

Figure 5 (b) compares similar illumination schemes, where the traditional illumination schemes were further broken down into the same session comparison as the corresponding diffuse illumination experiments. Here we see the traditional illumination experiments collected above a cluster of diffuse illumination experiments. Within the group of the traditional illumination experiments, comparisons from Sessions 1v6 and Sessions 4v5 have a similar mean ROC as well as overlapping error bars. However, the comparisons from Sessions 2v3 have a greater mean ROC and do not have error bars which overlap any other experiment. This variation could be due to the DCT method potentially employed by Algorithm 1, which cuts off certain frequencies which may be of interest in the diffused but not traditionally

illuminated images. In contrast, the diffuse illumination experiments have mean ROC true accept rates between 0.965 and 0.95 at a false accept rate of 0.002 and all error bars overlap all other error bars. Thus, these results are likely not statistically significantly different from one another. Figure 5 (c) further illustrates this result. Namely, that traditional illumination statistically significantly outperforms all the diffuse illumination experiments and that the diffuse illumination experiments perform at approximately the same recognition rate.

### 5.2. Algorithm 2

Algorithm 2 is a commercial package which performs both iris template extraction and matching [9]. Algorithm 2 reports an asymmetric similarity score which ranges from 0 to 9433, where 9433 indicates a perfect match. Asymmetric scoring means that given a pair of images, the algorithm will produce a different match depending on which image is used as the probe image. Figure 5 (d), (e), and (f) shows the results for each comparison experiment using Algorithm 2. The figure (d) depicts the results from comparing each week's traditional illumination data to the diffuse illuminated data. Considering only the mean ROC curves, without error bars, it appears that when comparing 25 degrees of diffusion to traditionally illuminated images the best results are seen given a false accept rate of 0.002. 30 degrees of diffusion then follows, with 20 degrees of diffusion comparisons at the lowest recognition rate. However, the error bars of all experiments overlap three or more other experiments, reducing the likelihood that these results are statistically significantly different from one another.

Figure 5 (e) depicts the results of same illumination scheme comparisons by week. Considering only the diffuse illumination system experiment's mean ROC results at false accept rate of 0.002, 25 degrees of diffusion performs the best, followed by 30 degrees of diffusion, and finally 20 degrees of diffusion. These results agree nicely with those from the initial same session experiments. Yet, the errors bars of the diffuse illumination experiments overlap, reducing the likelihood of a statistically significant difference. When looking at the traditional illumination comparison results, we find that two ROC curves perform almost perfectly, but the traditional Sessions 4v5 experiment performs with a true accept rate of about 0.999 at a false accept rate of 0.002. Sessions 1v6 and Sessions 2v3 have error bars which overlap with one another, but not those of other experiments. However, Sessions 4v5 performs about as well as 25 degrees of diffusion with error bars that completely overlap.

To better study the relationship between degrees of diffusion and traditional illumination, in Figure 5 (f) shows the combined recognition results of the traditionally illuminated dataset. Here, we see more clearly that traditional il-

illumination outperforms diffuse illumination. However, the error bars for the traditional illumination results somewhat overlap the 25 and 30 degrees of diffuse illumination ROC results. Thus, diffuse illumination does not appear to improve the recognition results when using Algorithm 2 for segmentation and matching.

### 5.3. Algorithm 3

Algorithm 3 is an in-house iris recognition software package based on a Daugman-like approach [8]. This algorithm reports a normalized fractional Hamming distance for each comparison. Scores are normalized based on the number of bits used in each comparison, and the resulting match scores range from 0 to approximately 1, where 0 represents a perfect match. The scores reported from Algorithm 3 are symmetric. This means that the score produced by using image A as the gallery image and image B as the probe image is the same as when using image B as the gallery and image A as the probe. Figure 5 (g), (h), and (i) shows the results of Algorithm 3 for this study. Figure 5 (g) shows the experimental results of same session traditional to diffuse illumination comparisons. These ROC results are less conclusive than that of the commercial algorithms. The sessions that use 30 degrees of diffusion cluster well, with a true accept rate of 0.98 at a false accept rate of 0.002. However, one of the sessions for both 20 and 25 degrees of diffusion fall above this cluster while the other falls below, providing a less conclusive ordering of traditional to diffuse illumination comparisons.

Figure 5 (h) depicts same illumination comparisons by session. When looking at the mean ROC results alone, at a false accept rate of 0.002, 20 degrees of diffusion performs the best, followed by 30 degrees of diffusion, 25 degrees of diffusion, then all the traditionally illuminated experiments. To more clearly analyze these results, the bottom figure shows the combination of the traditionally illuminated comparisons. Here, all of the diffuse illumination experiments outperform the traditional illumination experiment. Further, the traditional illumination ROC curves' error bars only overlap 25 degrees of diffusion before around a 0.0035 false accept rate. This shows that the diffuse illumination system, regardless of degree of diffusion, likely statistically significantly outperforms traditional illumination. However in contrast, the diffuse illumination experiments all have overlapping error bars, reducing the likelihood of a statistically significant difference in performance between degrees of diffusion.

## 6. Conclusions

This study aimed to accomplish three goals : (1) develop a diffuse illumination system based on an existing system, (2) determine if diffuse illumination can reduce specular highlights, and (3) analyze whether more diffuse illumina-

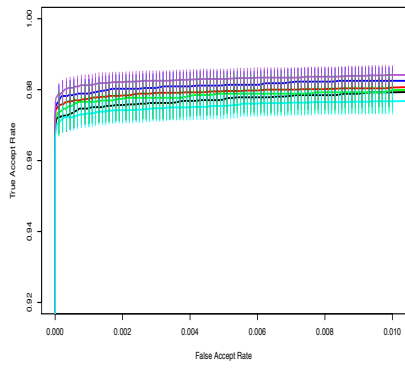
tion can aid in iris recognition. In our diffuse illumination system, we use various levels of external diffusing lenses in order to diffuse the illumination emitted by the LG IrisAccess 4000. By then analyzing the specular highlights within in the pupil and iris, we determined that we were successful in diffusing the illumination with this system. Additionally, the specular highlights from the pupil appear less prominent, allowing the possibility of increased segmentation accuracy and stronger template generation.

Given the creation of a diffuse illumination system based on the LG IrisAccess 4000 with reduced specular highlighting, various matching algorithms were then used to study the resulting diffused image templates. Some matchers showed no or little improvement when using diffuse illumination, as shown in Algorithm 1 and Algorithm 2's results. However, when using Algorithm 3, particular levels of diffusion showed statistically significant improvement over the traditional illumination system. Several quality metrics were studied for each matcher to further explain these variations in iris recognition performance.

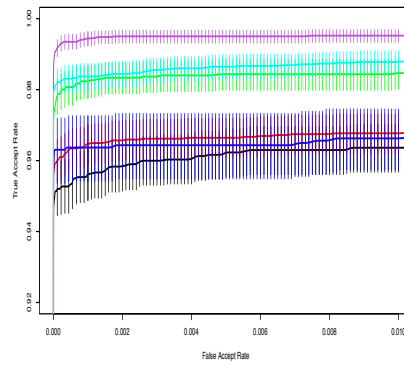
In conclusion, we have seen how a sensor's illumination scheme can be positively affected by an external factor (diffuse lenses). Although not all matchers used in this study showed improved performance, the reduction of specular highlights should prove to be beneficial for any segmentation algorithm.

## References

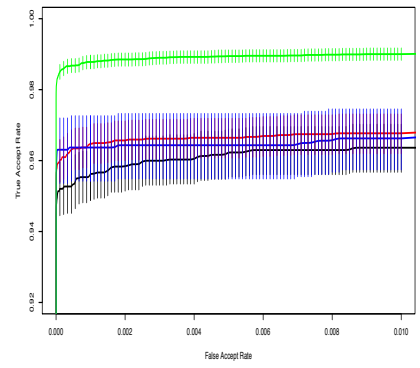
- [1] ICNIRP statment on light-emitting diodes (LEDs) and laser diodes: Implications for hazard assessment. *Health Physics*, 78(6):744–752, June 2000.
- [2] Edmund optics : Optics and optical instruments catalog. [www.edmundoptics.com](http://www.edmundoptics.com), 2009.
- [3] K. W. Bowyer, K. Hollingsworth, and P. J. Flynn. Image understanding for iris biometrics: A survey. *Computer Vision and Image Understanding*, 110(2):281–307, May 2008.
- [4] J. Daugman. High confidence visual recognition of persons by a test of statistical independence. *IEEE Transactions on Pattern Analysis and Machine Intelligence*, 15(11):1148–1161, November 1993.
- [5] A. K. Jain, A. Ross, and K. Nandakumar. *Introduction to Biometrics*, chapter Iris Recognition, pages 141–147. Springer Link, 2011.
- [6] Korea Testing Laboratory. IEC 60825-1 : Safety of Laser Products. Safety Report, September 2006.
- [7] LG Electronics U.S.A., Inc , Iris Technology Division. IrisAccess 4000 : next generation iris recognition system. [online] [www.irisid.com/download/brochure/IrisID-IrisAccess4000.pdf](http://www.irisid.com/download/brochure/IrisID-IrisAccess4000.pdf).
- [8] X. Liu, K. W. Bowyer, and P. Flynn. Experiments with an improved iris segmentation algorithm. In *Proceedings of the Fourth IEEE Workshop on Automatic Identification Technologies*, pages 118–123, 2005.
- [9] Neurotechnology. VeriEye SDK : iris identification for PC and web solutions. [online] <http://www.neurotechnology.com/verieye.html>, 2011.



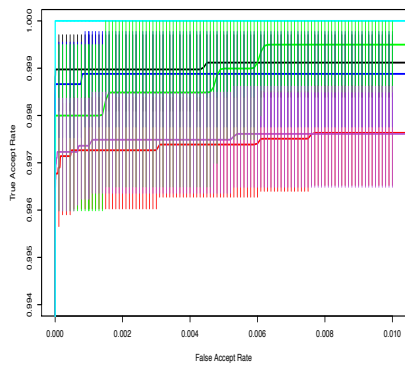
(a)



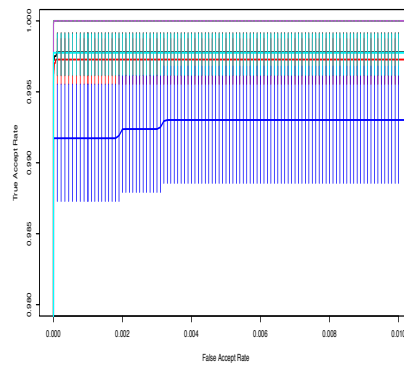
(b)



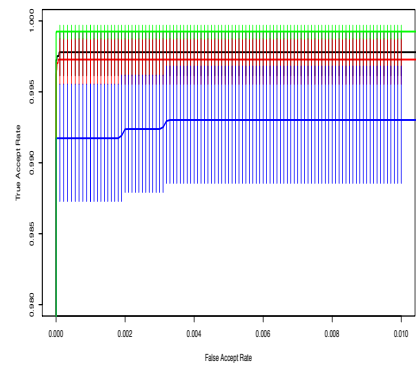
(c)



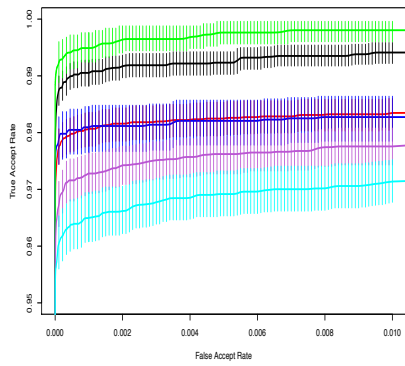
(d)



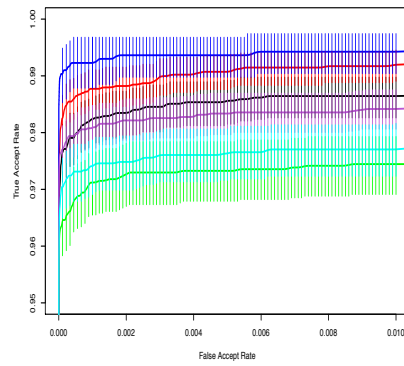
(e)



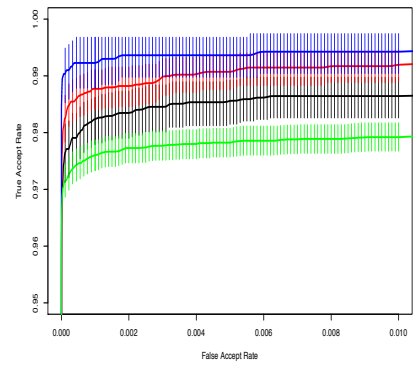
(f)



(g)



(h)



(i)

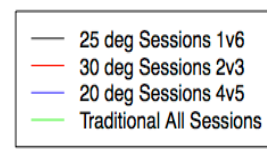
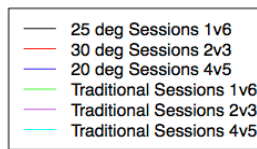
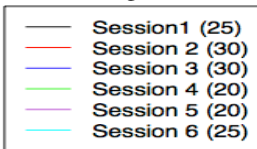


Figure 5. The results of Algorithm 1 are shown in (a), (b), and (c). The results of Algorithm 2 are shown in (d), (e), and (f). The results of Algorithm 3 are shown in (g), (h), and (i). The left most column shows the ROC curves resulting from comparisons of traditional and diffuse images from the same acquisition session. The middle column show results from comparisons from same illumination levels during different sessions. The rightmost column presents results from all comparisons using the same level of illumination during various sessions.